Langmuir

Article

pubs.acs.org/Langmuir

A Computational Study of Dicationic Ionic Liquids/CO_2 Interfaces

Song Li,[†] Wei Zhao,[†] Guang Feng,*[,†] and Peter T. Cummings[‡]

[†]State Key Laboratory of Coal Combustion, School of Energy and Power Engineering, Huazhong University of Science and Technology, Wuhan 430074, China

[‡]Department of Chemical and Biomolecular Engineering, Vanderbilt University, Nashville, Tennessee 37235, United States

Supporting Information

ABSTRACT: Recent studies on CO_2 capture using dicationic ionic liquids (DILs) demonstrated that DILs are promising absorbents for CO_2 uptake especially compared with monocationic ionic liquids (MILs) analogues, in which each cation carries single positive charge in contrast to two unit charges of a dication. However, DILs/CO_2 interfacial properties at the molecular level are still unknown. This work investigated the CO_2 absorption properties of representative DILs, 1-alkyl-3-dimethylimidazolium bis(trifluoromethylsulfonyl)imide, $[C_n(mim)_2](Tf_2N)_2$ (n = 3, 6, 12), using molecular dynamics (MD) simulations. The higher interfacial CO_2 density at DIL than that at MIL interfaces suggests the increased CO_2 interaction sites in DILs. The interfacial CO_2 density also exhibits an alkyl chain length dependence which decreases with the elongation of alkyl chain and proportionally correlates with the content of fluorine atoms at interfaces. Different alkyl chain orientations in DILs were illustrated in contrast to those of MILs; both DILs and CO_2 inside DILs exhibit lower diffusivity than MILs, in agreement with the stronger cation−anion binding energy of DILs. Moreover, DILs show a lower H_2O and N_2 uptake from flue gas compared with MILs, implicating the higher CO_2/H_2O and CO_2/N_2 selectivity.

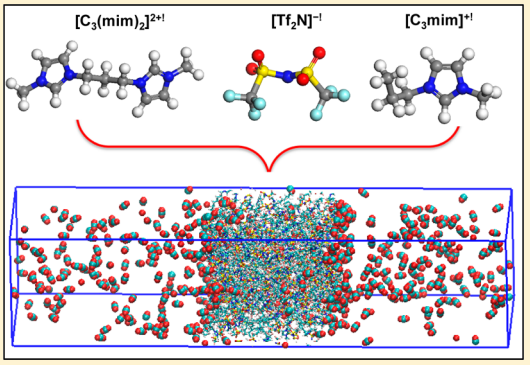

1. INTRODUCTION

CO_2 emission from the combustion of fossil fuels is one of the major causes of global warming, which highlights the important role of carbon capture and sequestration (CCS). Carbon capture is the most essential and expensive part of CCS due to its high energy consumption and low efficiency. Multiple techniques have been proposed for CO_2 capture, such as cryogenic distillation, membrane separation, and solvent absorption.[1] Among these strategies, solvent absorption, especially amine-containing solvents, was proposed as the most applicable technique due to its high energy efficiency and facile operation.[2] However, the current amine-containing solvents used (e.g., monoethanolamine and KS-1) have drawbacks including high energy consumption, high volatility, poor stability, and so on.[3,4] The emerging room temperature ionic liquids (RTILs) eliminate such shortcomings and show selective absorption of CO_2.[5] RTILs consisting solely of organic cations and organic/inorganic anions exhibit low volatility as well as high thermal/electrochemical stability. In addition, RTILs are more environmental-friendly compared to conventional organic solvents, and most of them can be regenerated easily in comparison with amine aqueous solvents. Another hallmark property of RTILs is their tunability by a variety of combinations of cations and anions, which renders the structural diversity of RTILs with potential application for CO_2 capture.[6]

Since the first investigation of RTILs as CO_2 absorption media in 1999,[7] lots of experimental and theoretical studies on the CO_2 capture capability of RTILs have been reported. The crucial structure−property relationships regarding CO_2 absorption capability of RTILs have also been addressed. For instance, Maginn's group has designed a new type of aprotic heterocyclic anions (AHA)-containing ionic liquids for CO_2 capture, which exhibit high capacity, low viscosity, and chemical tunability.[8] Their water solubility was also investigated recently.[9] These studies indicate the feasibility of designing task-specific ionic liquids for CO_2 capture.

It is reported that CO_2 uptake by RTILs relies on the solubility of CO_2 in RTILs and CO_2 solubility in RTILs is dominated by the interaction strength of CO_2 with anions,[5] which increases with the increase of the content of fluorine in anions due to the enhanced binding energy.[10] Recent studies by Babarao and Gupta et al. demonstrated that CO_2 solubility is governed by the binding energy of cation−anion rather than CO_2−anion.[11,12] Aki et al. investigated the effects of alkyl chain length of cations on CO_2 solubility by experimental measurement, in which it was found that CO_2 solubility was slightly increased with the elongation of alkyl chain.[10] The same tendency was also observed in atomistic Monte Carlo simulations.[13] To our knowledge, all the reported studies on carbon capture by RTILs are concentrated on monocationic ionic liquids (MILs), where each cation carries single unit charge. Dicationic ionic liquids (DILs) are new members of RTILs family, in which each cation carries two unit charges.

Received: December 15, 2014
Revised: February 1, 2015

DOI: 10.1021/la5048563
Langmuir XXXX, XXX, XXX−XXX

DILs have high thermal stability[14] and low heterogeneity in contrast to counterpart MILs.[15] In our previous work, we have investigated their distinctive structural organization[15] and electrochemical performance as electrolytes in supercapacitors;[16] however, the CO_2 sorption capability of DILs is little known, especially compared to that of MILs. Recently, Zhang et al. observed the enhanced CO_2 uptake by DILs, 1,2-bis(3-methylimidazolium-1-yl)ethane imidazolate ([Bis(mim)C_2]-[Im]$_2$), and 1,4-bis(3-methylimidazolium-1-yl)butane imidazolate ([Bis(mim)C_4]-[Im]$_2$), in which the CO_2 uptake by DILs is twice that of their MIL analogues.[17] Similarly, Hojniak et al. reported that DILs-incorporated membranes exhibited the enhanced CO_2/N_2 selectivity and adsorption capability in comparison with MILs-incorporated membrane, which was ascribed to the increased CO_2 interaction sites in DILs.[18] These studies have imparted the potential application of DILs for CO_2 capture.

In this work, from a viewpoint of modeling, we investigated the CO_2/DILs interfacial phenomena by molecular dynamics (MD) simulations of CO_2/DILs (1-alkyl-3-dimethylimidazolium bis(trifluoromethylsulfonyl)imide, $[C_n(mim)_2](Tf_2N)_2$ (n = 3, 6, 12) and CO_2/MILs ($[C_n mim][Tf_2N]$ (n = 3, 6)) interfaces. Both interfacial structural and dynamical properties of CO_2/DILs and CO_2/MILs were compared, and their interfacial behaviors at flue gas/*RT*ILs were also analyzed. Additionally, the binding energies of dication−anion and monocation−anion were calculated in order to estimate the interaction strength of ion pairs via *ab initio* calculation.

2. METHODOLOGY

Classical Molecular Dynamics Simulation. The force field used for dications $[C_n(mim)_2]^{2+}$ (n = 3, 6, 12) was adapted from the all-atom model developed by Yeganegi et al.[19] The force fields for monocations and anions were taken from the study of Lopes' group.[20] Force field parameters for CO_2 and H_2O were taken from Shi et al.'s study,[13] and those for N_2 and O_2 were from Arora et al.'s work.[21] All the C−H bonds were constrained using the LINCS algorithm[22] during the simulation, and a 1.5 nm cutoff was used for van der Waals interactions. Long-range electrostatic interactions were processed using the particle mesh Ewald (PME) method.[23] An RTIL box consisting of 100 ion pairs with the size of approximately 4.12 nm × 4.12 nm × 4.12 nm was equilibrated at 350 K and 1 bar for 6 ns, followed with a 12 ns production run. The CO_2/RTILs interfaces were created by placing two cubic boxes of 216 CO_2 molecules above and below the RTIL slab, respectively. Then canonical ensemble MD simulation was conducted at 350 K to study the interfacial absorption behavior of CO_2. A model of flue gas box containing 150 N_2, 20 CO_2, 20 H_2O, and 10 O_2 was also used in order to obtain the interfacial properties of flue gas/RTILs interfaces. The periodic boundary condition (PBC) was applied in three dimensions. All simulations in this work were performed using MD package Gromacs.[24]

The diffusion coefficient was calculated according to the Einstein relation

$$D = \lim_{t\to\infty} \frac{1}{6t}\langle [r_i(t) - r_i(0)]^2 \rangle \quad (1)$$

where D is the diffusion coefficient, t is time, $r_i(t)$ is the position of particle i at time t, and $r_i(0)$ is the initial position of particle i.

The averaged number density profiles were calculated along the direction perpendicular to the CO_2/RTILs interfaces by binning method. The orientational order parameter of RTILs and CO_2 was described by the second-order Legendre polynomials defined in the equation

$$\langle P_2 \rangle = \left\langle \frac{1}{2}(3\cos^2\theta - 1) \right\rangle \quad (2)$$

where $\langle P_2 \rangle$ is the average orientational order parameter and θ is the angle formed by alkyl chain vector with the normal to $[C_n(mim)_2](Tf_2N)_2$ /CO_2 (n = 3, 6, 12) interfaces.

***Ab Initio* Calculation.** Geometry optimizations of dication $[C_3(mim)_2]^{2+}$, monocation $[C_3mim]^+$, and anion $[Tf_2N]^-$ were implemented at the B3LYP level using the 6-311+G(d, p) basis set in Gaussian09.[25] In order to calculate the binding energy between cations and anions, the cation−anion complex was also optimized. The different relative positions of the anion around the cation were tried to locate the lowest potential energy surface. Single point energy followed by frequency calculation was carried out at MP2 level. To compensate for basis set superposition error, the obtained binding energy of cation−anion was corrected by the counterpoise method.[26]

3. RESULTS AND DISCUSSION

IL + CO_2 System. In order to obtain the interfacial structural information on RTIL/CO_2 systems, the number density profiles of CO_2 across dicationic $[C_n(mim)_2](Tf_2N)_2$ and monocationic $[C_n mim][Tf_2N]$ slabs were analyzed, based on the center of mass (CoM) of ions, in Figures 1 and 2. It is

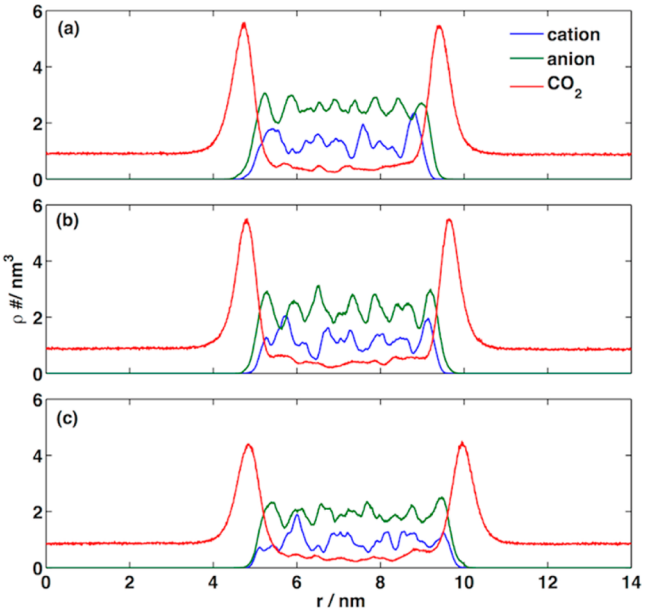

Figure 1. Number density profiles of center of mass of cations, anions, and CO_2 across $[C_n(mim)_2](Tf_2N)_2/CO_2$ systems for n = 3 (a), n = 6 (b), and n = 12 (c) at 350 K.

remarked that the anion density is twice that of cations of $[C_n(mim)_2](Tf_2N)_2$ in Figure 1, which is the feature of DILs since the molar ratio of anions in DILs is twice that of cations. Whereas, monocationic $[C_n mim][Tf_2N]$ in Figure 2 exhibits similar density for cations and anions. In contrast to cation CoM-based density profile, the number density profiles based on the CoM of imidazolium ring of dications and monocations were computed and shown in Figures S1 and S2. Once can find that DILs exhibit similar cation and anion densities because of

DOI: 10.1021/la5048563
Langmuir XXXX, XXX, XXX−XXX

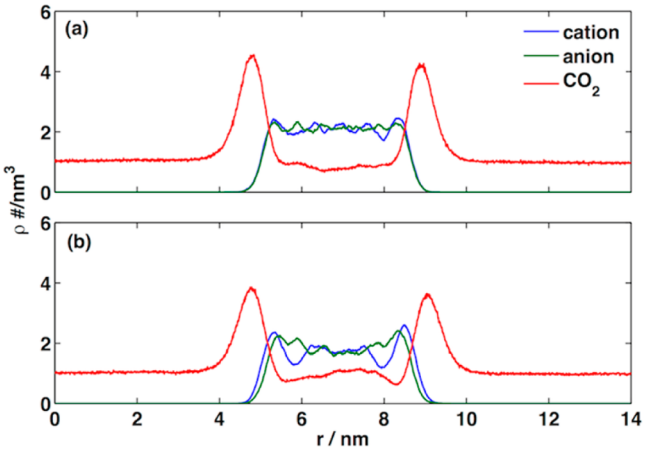

Figure 2. Number density profiles of center of mass of cations, anions, and CO_2 across $[C_n\text{mim}][Tf_2N]/CO_2$ systems for $n = 3$ (a) and $n = 6$ (b) at 350 K.

the same number density of imidazolium rings and anions in DILs. Additionally, different from the dication CoM-based number density profiles, the imidazolium ring CoM density overlaps with the anion density at IL/CO_2 interfaces, which is because the imidazolium ring carries most of the positive charge in the cation and closely interacts with the anion. Moreover, there is more significant fluctuation observed in density of DILs (Figure 1) than MILs (Figure 2), and the fluctuation becomes more visible with the elongation of alkyl chain in cations, which is probably attributed to the large sizes of dications and their complicate geometries in comparison with those of MILs.

Moreover, the absorbed layer of CO_2 formed at RTILs interfaces has been reported in many computational studies, which is also observed in dicationic $[C_n(\text{mim})_2](Tf_2N)_2/CO_2$ systems (Figure 1). The two absorbed CO_2 layers with almost equivalent density at interfaces were identified due to the strong CO_2–RTIL interactions. It is known that the CO_2–RTIL interaction is dominated by anions,[5] as evidenced by the density profile shown in Figure 1, in which the interfacial anions are closer to CO_2 than cations, resulting in negatively charged region at interfaces and positively charged region resulting from the accumulation of CO_2 (Figure S3). However, this tendency cannot be differentiated according to the number density profile of center of mass of ions for MILs in Figure 2. Therefore, the number density profile of specific atoms in cations and anions was analyzed in Figure 3. It is obvious that fluorine atoms in anions closely interact with CO_2 in contrast to other atoms due to the stronger binding energy, which agrees with previous report.[10] This phenomenon is substantiated in both dicationic $[C_3(\text{mim})_2](Tf_2N)_2/CO_2$ (Figure 3a) and monocationic $[C_3\text{mim}][Tf_2N]/CO_2$ (Figure 3b). Another phenomenon noticed is that the number density of CO_2 inside MILs (Figure 2) is higher than that inside DILs (Figure 1), which is probably ascribed to the high viscosity of DILs that requires long time for CO_2 to interact with all binding sites of DILs.

It should also be noted that the number density of CO_2 in absorbed layer decreases with the increase of alkyl chain length, similar to the observation in monocationic $[C_n\text{mim}][Tf_2N]/CO_2$ system in Figure 2. Since CO_2-RTILs interactions are dominated by anions, especially fluorine atoms in $[Tf_2N]^-$, we analyze the fluorine density profile of anions across RTILs with different alkyl chain lengths in Figure 4. The fluorine density at interfaces decreases with the increasing chain length in both DILs (Figure 4a) and MILs (Figure 4b), corresponding to the decreased absorbed CO_2 density. This phenomenon probably indicates that the content of fluorine at RTILs/CO_2 interfaces plays a crucial role in determining the density of CO_2 in the adsorbed layer. It is noteworthy that in general interfacial fluorine density in dicationic $[C_n(\text{mim})_2](Tf_2N)_2$ is higher than their monocationic counterparts, which can also be ascribed to the higher anion density in DILs.

It is instructive to deliberate the orientation changes of both RTILs and CO_2 at interfaces, especially for dicationic $[C_n(\text{mim})_2](Tf_2N)_2/CO_2$, which may exhibit dissimilar behav-

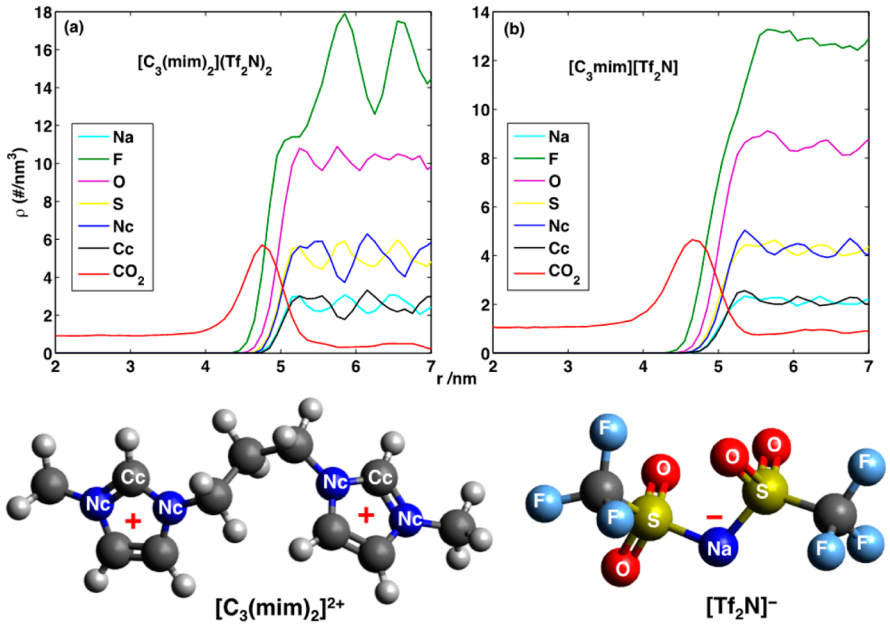

Figure 3. Atomic number density profiles of cations, anions, and CO_2 across $[C_3(\text{mim})_2](Tf_2N)_2$ (a) and $[C_3\text{mim}][Tf_2N]$ (b) at 350 K. The atoms were specified in the molecular models of $[C_3(\text{mim})_2]^{2+}$ and $[Tf_2N]^-$ in the bottom.

DOI: 10.1021/la5048563
Langmuir XXXX, XXX, XXX–XXX

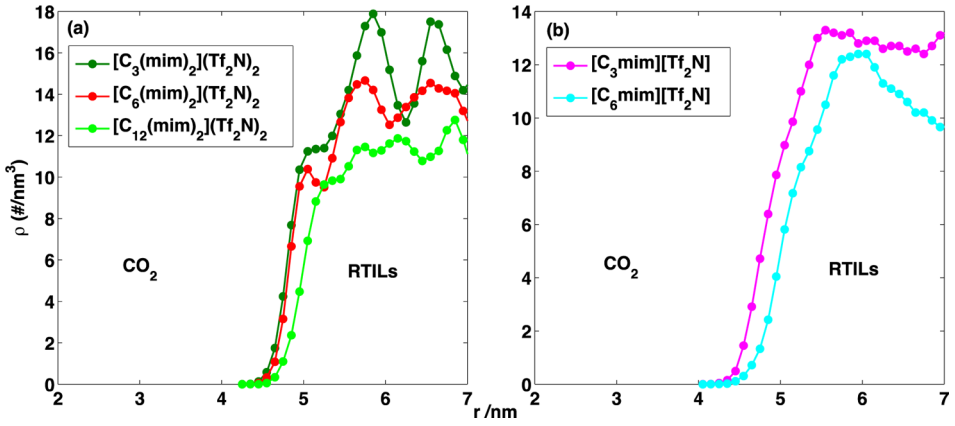

Figure 4. Fluorine number density profiles of $[C_n(mim)_2](Tf_2N)_2$ (n = 3, 6, 12) (a) and $[C_nmim][Tf_2N]$ (n = 3, 6) (b) at 350 K.

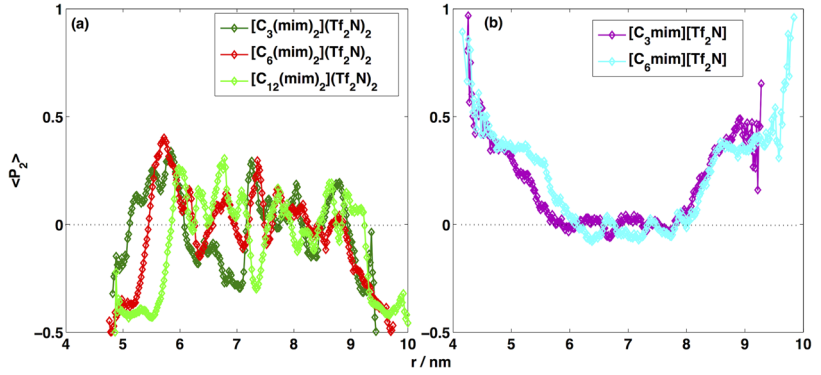

Figure 5. Orientational order parameter of the angle formed by alkyl chain vector with the normal to $[C_n(mim)_2](Tf_2N)_2$ /CO_2 (n = 3, 6, 12) interfaces (a) and $[C_nmim][Tf_2N]/CO_2$ (n = 3, 6) interfaces (b) at 350 K.

iors to monocationic $[C_nmim][Tf_2N]/CO_2$. First of all, the orientation order parameter, $\langle P_2 \rangle$, of alkyl chains in cations at IL/gas interfaces is presented in Figure 5. For dicationic $[C_n(mim)_2](Tf_2N)_2$, $\langle P_2 \rangle$ of linkage alkyl chain at interfaces is close to −0.5, corresponding to 90° with the normal of interfaces or parallel to the interface. This tendency is different from free alkyl chains of monocationic $[C_nmim][Tf_2N]$ shown in Figure 5b, which stretch out into gas phase and tend to be perpendicular to interfaces. This observation has been reported in previous studies on MILs/CO_2 interfaces.[12,13,27] Such a difference in the alkyl chain orientation of interfacial DILs and MILs is probably because the alkyl chain of dications is connected with two positively charged imidazolium rings, which increases the electrostatic interaction within DILs and restricts the flexibility of alkyl chains. The imidazolium planes of both dicationic $[C_n(mim)_2](Tf_2N)_2$ and monocationic $[C_nmim][Tf_2N]$ at interfaces prefer to parallelize with RTILs/CO_2 interfaces (Figure S4). Such an orientation is in agreement with many reports on RTILs−vacuum interfaces,[28−30] although it may not be the same for all the types of ionic liquids.

The orientation of CO_2 is defined as the tilt angle formed by O−O vector of CO_2 and the normal to the interfaces. The result is presented in the form of orientational order parameter shown in Figure 6. It was found that, from gas phase to the interface, $\langle P_2 \rangle$ value is decreased from 0 to ∼ −0.1 for both dicationic and monocationic RTILs/CO_2 systems, suggesting CO_2 slightly tilted toward the interfaces as approaching liquid phase in Figure 6c. The insignificant tendency in CO_2 orientation is also reported in previous study,[31] in which CO_2 exhibits slight tendency to lie flat on liquid surface due to the strengthened interaction of RTILs−CO_2 at interfaces. In addition, the dramatic fluctuation of $\langle P_2 \rangle$ for CO_2 inside DILs (Figure 6a) was observed in contrast to that inside MILs (Figure 6b), and the oscillation decreases with chain length. Overall, there is a more diverse range of CO_2 orientations in DILs than MILs, which may correlate with the spatial heterogeneity observed in DILs and MILs. According to our previous study,[15] free alkyl chains in MILs are relatively easy to aggregate, and thus the segregation of polar and nonpolar domains is observed. However, such segregation in DILs is not significant due to the strong electrostatic interactions, which indicates that the distinctive degrees of spatial heterogeneity in DILs and MILs may contribute to dissimilar orientations of CO_2 inside. This deserves further investigation in future work.

In addition, the diffusivity of CO_2 inside RTILs was computed and listed in Table 1. For MILs, the diffusion coefficient of CO_2 in MILs decreases with the increase in chain length of cations, similar to the trend of cation/anion diffusion, suggesting that the diffusion of CO_2 inside RTILs is dependent on the diffusion of RTILs as reported in a previous study.[32] For DILs, the CO_2 diffusion coefficient also decreases with the elongation of alkyl chain and CO_2 diffusion is slower than that in MILs by 1−2 orders of magnitude, which can be attributed to the high viscosity[33] and longer ion pair lifetime of DILs.[34] The ion diffusion of DILs exhibits chain-length independence, consistent with reported chain length-dependent viscosity of bulk DILs.[33]

IL + Flue Gas System. In practice, the separation of CO_2 from flue gas including N_2, H_2O, and O_2 is paramount for CO_2

DOI: 10.1021/la5048563
Langmuir XXXX, XXX, XXX−XXX

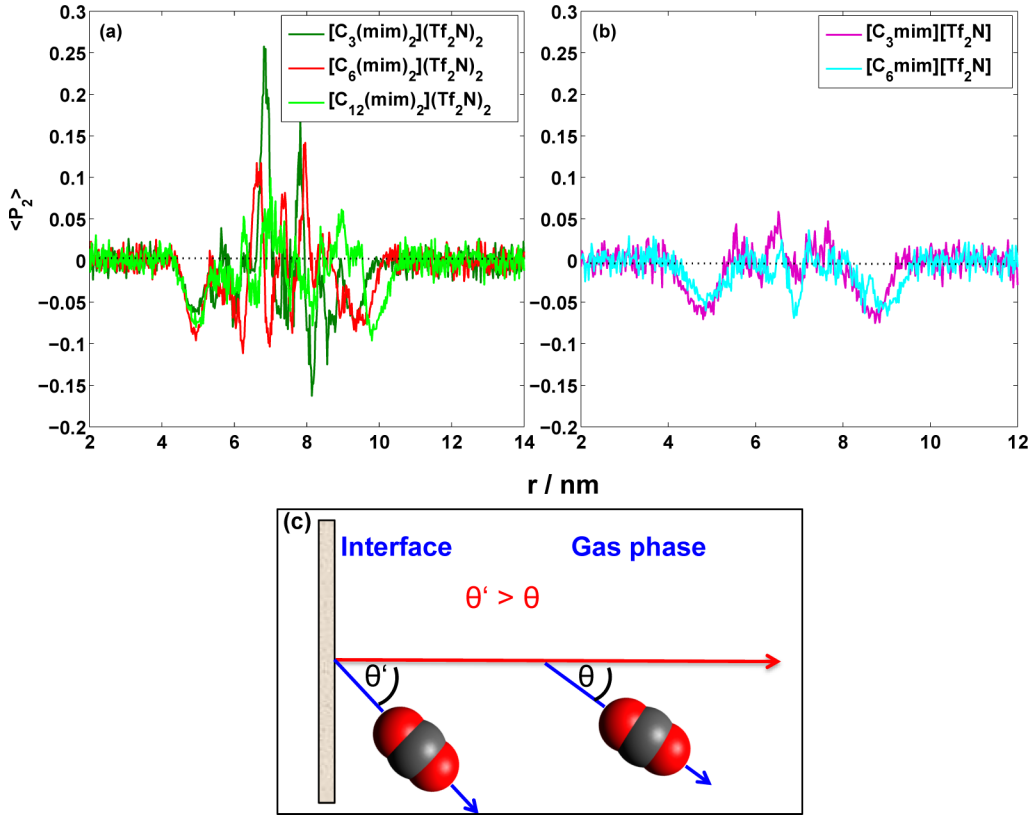

Figure 6. Orientation order parameter of the angle formed by O−O vector in CO_2 with the normal of RTIL/CO_2 interface for $[C_n(mim)_2](Tf_2N)_2$ (n = 3, 6, 12) (a) and $[C_n mim][Tf_2N]$ (n = 3, 6) (b) at 350 K. The schematic representation of the variation in orientation of CO_2 from bulk gas phase toward interfacial absorbed layer.

Table 1. Diffusion Coefficients (m^2/s) of CO_2, Cations, and Anions at CO_2−RTIL Interfaces

RTIL name	D_{CO_2} inside RTILs[a]	D_{cation} inside RTILs	D_{anion} inside RTILs
$[C_3(mim)_2](Tf_2N)_2$	4.83×10^{-10}	2.50×10^{-10}	3.00×10^{-10}
$[C_6(mim)_2](Tf_2N)_2$	4.60×10^{-10}	1.67×10^{-10}	1.50×10^{-10}
$[C_{12}(mim)_2](Tf_2N)_2$	4.30×10^{-10}	1.83×10^{-10}	1.83×10^{-10}
$[C_3mim][Tf_2N]$	1.08×10^{-8}	8.33×10^{-10}	9.50×10^{-10}
$[C_6mim][Tf_2N]$	4.76×10^{-9}	4.83×10^{-10}	5.17×10^{-10}

[a] D_{CO_2} inside RTILs denoted the pseudobulk region of RTILs with a width of 2 nm in the middle of slab.

capture, by which CO_2 can be selectively removed from gas mixture. The ideal RTIL candidates for CO_2 capture should not only exhibit high CO_2 uptake but also high selectivity toward CO_2 in the presence of other gas molecules. In this study, we explored the absorption of flue gas consisting of N_2, CO_2, H_2O, and O_2 at the molar ratio of 15:2:2:1 by both dicationic $[C_3(mim)_2](Tf_2N)_2$ and monocationic $[C_3mim][Tf_2N]$. The number density profiles of the four components in flue gas are shown in Figure 7 and show that all four types of gases form absorbed layers at interfaces, and N_2 exhibits the highest density at $[C_3mim][Tf_2N]$ interface followed by CO_2, H_2O, and O_2. Whereas, the density order at $[C_3(mim)_2](Tf_2N)_2$ interface follows N_2 > H_2O > CO_2 > O_2. The significant discrepancy in the densities of H_2O inside $[C_3(mim)_2](Tf_2N)_2$ and $[C_3mim][Tf_2N]$ is also noticed, implicating the relatively hydrophobic nature of dicationic $[C_3(mim)_2](Tf_2N)_2$ in contrast to $[C_3mim][Tf_2N]$. Such a discrepancy is even more evident in the 2-D density map of absorbates shown in Figure 8.

Among these gas molecules, both $[C_3(mim)_2](Tf_2N)_2$ and $[C_3mim][Tf_2N]$ exhibit the highest uptake of H_2O and monocationic $[C_3mim][Tf_2N]$ shows much higher H_2O absorption than dicationic $[C_3(mim)_2](Tf_2N)_2$. Whereas, there is no obvious difference in CO_2 uptake of dicationic $[C_3(mim)_2](Tf_2N)_2$ and monocationic $[C_3mim][Tf_2N]$. Interestingly, there is very little N_2 uptake observed in dicationic $[C_3(mim)_2](Tf_2N)_2$ (e.g., the average number of N_2 molecules in the IL slab between 6 and 8 nm is 0.69). However, a considerable number of absorbed N_2 molecules are present in monocationic $[C_3mim][Tf_2N]$ (e.g., the average number of N_2 molecules in the IL slab between 6 and 8 nm is 1.43). Such a tendency is in agreement with previous experimental report that DILs-incorporated membrane exhibits higher CO_2 /N_2 selectivity than MILs-incorporated one due to the decreased N_2 permeability resulted from the reduced DILs-N_2 affinity and increased CO_2 interaction sites of DILs.[18] In addition, dicationic $[C_3(mim)_2](Tf_2N)_2$ shows higher O_2 absorption than monocationic $[C_3mim][Tf_2N]$. However, this is not a big concern for the use of $[C_3(mim)_2](Tf_2N)_2$ in CO_2 capture since (1) the molar ratio of O_2 in flue gas is extremely low (5%) and (2) the low solubility and weak interaction of O_2 with ionic liquids.[35]

Optimized Ion Pairs and Binding Energy. Babarao and Gupta et al.'s studies on nitrile-based ionic liquids have demonstrated that CO_2 solubility in ionic liquids is governed by the cation−anion binding energy rather than anion−CO_2 binding energy, which increases with the decreasing of cation−anion binding energy.[11,12] In this work, since DILs

DOI: 10.1021/la5048563
Langmuir XXXX, XXX, XXX−XXX

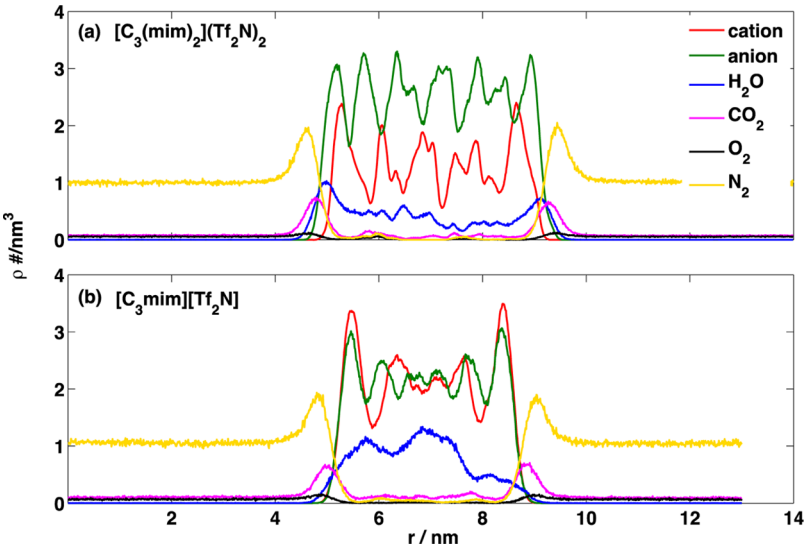

Figure 7. Number density profiles of cations, anions, and flue gas across RTILs/flue gas interfaces for $[C_3(mim)_2](Tf_2N)_2$ (a) and $[C_3mim][Tf_2N]$ (b).

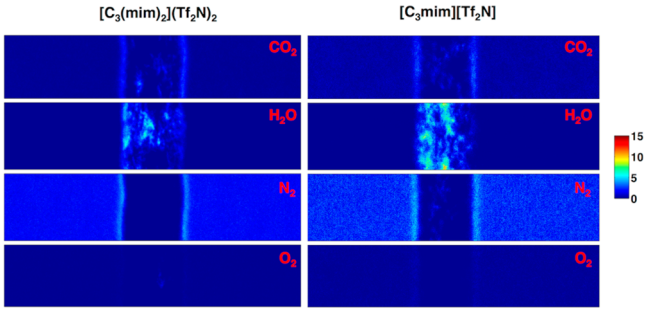

Figure 8. 2-D number density maps of CO_2, H_2O, N_2, and O_2 in $[C_3(mim)_2](Tf_2N)_2$ /flue gas (left) and $[C_3mim][Tf_2N]$/flue gas systems (right).

and MILs share the same type of anions, the anion−CO_2 binding energy is assumed to be identical for dicationic $[C_3(mim)_2](Tf_2N)_2$ and monocationic $[C_3mim][Tf_2N]$. Thus, the cation−anion binding energy is critical for determining CO_2 solubility. The cation−anion configurations for DILs and MILs were optimized, and the corresponding binding energy was estimated using *ab initio* calculation as shown in Figure 9. It should be noticed that there is hydrogen bond formed between the hydrogen in cations and oxygen in anions in the optimized complex. It is obvious that two hydrogen bonds formed in the

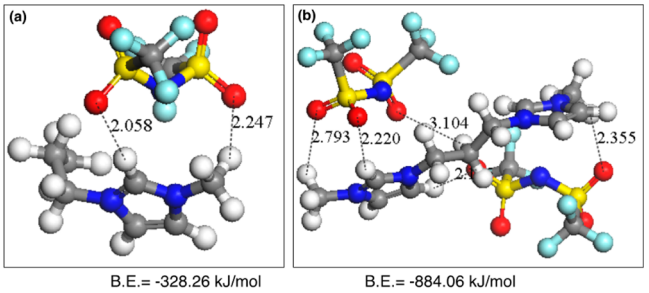

Figure 9. Optimized structures of (a) monocationic $[C_3mim]^+$−$[Tf_2N]^-$ and (b) dicationic $[C_3(mim)_2]^{2+}$−2$[Tf_2N]^-$ complex with hydrogen bond formed (in Å) and cation−anion binding energy (in kJ/mol).

$[C_3mim]^+$−$[Tf_2N]^-$ complex, while approximately six hydrogen bonds were observed in dicationic $[C_3(mim)_2](Tf_2N)_2$, suggesting the stronger interaction between dication $[C_3(mim)_2]^{2+}$−anions than monocation $[C_3mim]^+$−anions.

The cation−anion binding energy of MIL, $[C_3mim][Tf_2N]$, is −328.26 kJ/mol as computed from *ab initio* calculation, whereas the cation−anion binding energy of DIL, $[C_3(mim)_2](Tf_2N)_2$, is −884.06 kJ/mol, more than twice that of $[C_3mim][Tf_2N]$. According to Babarao and Gupta et al.'s reports, cation−anion binding energy dominated CO_2 solubility in ionic liquids; specifically, the higher the binding energy, the lower CO_2 solubility.[11,12] The high cation−anion binding energy of $[C_3(mim)_2](Tf_2N)_2$ may indicate the lower solubility of CO_2 inside DILs than in MILs, as shown in the number density profiles of CO_2 inside DILs and MILs in Figures 1 and 2. The higher cation−anion binding energy of DILs also explains the lower diffusion coefficients of CO_2 in DILs compared with those in MILs (Table 1). The low CO_2 solubility and diffusivity in DILs observed in simulation are probably due to the high viscosity of DILs studied. However, in experimental studies, the higher CO_2 uptake was observed in DILs with reactive cations,[17] and the higher CO_2/N_2 selectivity was reported by using DILs incorporated membranes,[18] which overcome the high viscosity or slow dynamics of DILs. Therefore, the redesign of DILs by replacing ions and/or modifying chemical structure to tune the physiochemical properties of DILs may improve their performance as CO_2 adsorbents.

4. CONCLUSION

Ionic liquids are promising absorbents for CO_2 capture, which exhibit selective affinity toward CO_2. Dicationic ionic liquids (DILs) are recently reported as prospective alternatives of CO_2 absorbents due to the increased CO_2 binding sites present in DILs. Previous studies have demonstrated that DILs shown several advantages over monocationic counterparts, such as increased CO_2 binding sites[17] and high CO_2 selectivity.[18] This work exploited the DIL−CO_2 interfacial properties using MD simulations. The chain-length-dependent CO_2 accumulation ability at interfaces was related to interfacial fluorine content, as evidenced by atomic number density profiles. We also found

DOI: 10.1021/la5048563
Langmuir XXXX, XXX, XXX−XXX

that DILs exhibited different orientations at interfaces from MILs, resulting from the distinct geometries and compositions of DILs. Comparison of DIL/flue gas and MIL/flue gas interfaces demonstrates that less water is absorbed by DILs in comparison to MILs. Although DILs exhibit a slow diffusivity in comparison with MILs as suggested by the higher cation−anion binding energy of DILs, they are proposed as more promising CO_2 absorbent candidates because the redesign of DILs will overcome such shortcoming and enhance CO_2 uptake as reported in Zhang et al.'s study.[17] This study provides a fundamental understanding of DILs−CO_2 interfacial properties, which may motivate more relevant investigations for the development of DILs-based CO_2 absorbents.

■ ASSOCIATED CONTENT

Supporting Information

Figures S1−S4. This material is available free of charge via the Internet at http://pubs.acs.org.

■ AUTHOR INFORMATION

Corresponding Author

*E-mail: gfeng@hust.edu.cn (G.F.).

Notes

The authors declare no competing financial interest.

■ ACKNOWLEDGMENTS

G.F. and W.Z. acknowledge the funding support from National Natural Science Foundation of China (51406060) and Natural Science Foundation of Hubei Province of China (2014CFA089). P.T.C. thanks the support by Fluid Interface Reactions, Structures, and Transport (FIRST) Center, an Energy Frontier Research Center funded by the U.S. Department of Energy, Office of Science, Office of Basic Energy Sciences. The work was partially carried out at National Supercomputer Center in Tianjin, and the calculations were performed on TianHe-1 (A). Computations were in part performed at the National Energy Research Scientific Computing Center, which is supported by the Office of Science of the U.S. Department of Energy under Contract DE-AC02-05CH11231.

■ REFERENCES

(1) Smit, B.; Reimer, J. A.; Oldenburg, C. M.; Bourg, I. C. *Introduction to Carbon Capture and Sequestration*; Imperial College Press: London, 2014; Vol. *1*.

(2) Rochelle, G. T. Amine Scrubbing for CO_2 Capture. *Science* **2009**, *325*, 1652−1654.

(3) Karadas, F.; Atilhan, M.; Aparicio, S. Review on the Use of Ionic Liquids (Ils) as Alternative Fluids for CO_2 Capture and Natural Gas Sweetening. *Energy Fuels* **2010**, *24*, 5817−5828.

(4) Yu, C.-H.; Huang, C.-H.; Tan, C.-S. A Review of CO_2 Capture by Absorption and Adsorption. *Aerosol Air Qual. Res.* **2012**, *12*, 745−769.

(5) Cadena, C.; Anthony, J. L.; Shah, J. K.; Morrow, T. I.; Brennecke, J. F.; Maginn, E. J. Why Is CO_2 So Soluble in Imidazolium-Based Ionic Liquids? *J. Am. Chem. Soc.* **2004**, *126*, 5300−5308.

(6) Zhang, X. P.; Zhang, X. C.; Dong, H. F.; Zhao, Z. J.; Zhang, S. J.; Huang, Y. Carbon Capture with Ionic Liquids: Overview and Progress. *Energy Environ. Sci.* **2012**, *5*, 6668−6681.

(7) Blanchard, L. A.; Hancu, D.; Beckman, E. J.; Brennecke, J. F. Green Processing Using Ionic Liquids and CO_2. *Nature* **1999**, *399*.

(8) Gurkan, B.; Goodrich, B. F.; Mindrup, E. M.; Ficke, L. E.; Massel, M.; Seo, S.; Senftle, T. P.; Wu, H.; Glaser, M. F.; Shah, J. K.; Maginn, E. J.; Brennecke, J. F.; Schneider, W. F. Molecular Design of High Capacity, Low Viscosity, Chemically Tunable Ionic Liquids for CO_2 Capture. *J. Phys. Chem. Lett.* **2010**, *1*, 3494−3499.

(9) Wu, H.; Maginn, E. J. Water Solubility and Dynamics of CO_2 Capture Ionic Liquids Having Aprotic Heterocyclic Anions. *Fluid Phase Equilib.* **2014**, *368*, 72−79.

(10) Aki, S. N. V. K.; Mellein, B. R.; Saurer, E. M.; Brennecke, J. F. High-Pressure Phase Behavior of Carbon Dioxide with Imidazolium-Based Ionic Liquids. *J. Phys. Chem. B* **2004**, *108*, 20355−20365.

(11) Babarao, R.; Dai, S.; Jiang, D. E. Understanding the High Solubility of CO_2 in an Ionic Liquid with the Tetracyanoborate Anion. *J. Phys. Chem. B* **2011**, *115*, 9789−9794.

(12) Gupta, K. M.; Jiang, J. W. Systematic Investigation of Nitrile Based Ionic Liquids for CO_2 Capture: A Combination of Molecular Simulation and Ab Initio Calculation. *J. Phys. Chem. C* **2014**, *118*, 3110−3118.

(13) Shi, W.; Maginn, E. J. Atomistic Simulation of the Absorption of Carbon Dioxide and Water in the Ionic Liquid 1-N-Hexyl-3-Methylimidazolium Bis(Trifluoromethylsulfonyl)Imide ([Hmim]-[Tf_2N]. *J. Phys. Chem. B* **2008**, *112*, 2045−2055.

(14) Anderson, J. L.; Ding, R. F.; Ellern, A.; Armstrong, D. W. Structure and Properties of High Stability Geminal Dicationic Ionic Liquids. *J. Am. Chem. Soc.* **2005**, *127*, 593−604.

(15) Li, S.; Feng, G.; Banuelos, J. L.; Rother, G.; Fulvio, P. F.; Dai, S.; Cummings, P. T. Distinctive Nanoscale Organization of Dicationic Versus Monocationic Ionic Liquids. *J. Phys. Chem. C* **2013**, *117*, 18251−18257.

(16) Li, S.; Van Aken, K. L.; McDonough, J. K.; Feng, G.; Gogotsi, Y.; Cummings, P. T. The Electrical Double Layer of Dicationic Ionic Liquids at Onion-Like Carbon Surface. *J. Phys. Chem. C* **2014**, *118*, 3901−3909.

(17) Zhang, Y.; Wu, Z. K.; Chen, S. L.; Yu, P.; Luo, Y. B. CO_2 Capture by Imidazolate-Based Ionic Liquids: Effect of Functionalized Cation and Dication. *Ind. Eng. Chem. Res.* **2013**, *52*, 6069−6075.

(18) Hojniak, S. D.; Khan, A. L.; Holloczki, O.; Kirchner, B.; Vankelecom, I. F. J.; Dehaen, W.; Binnemans, K. Separation of Carbon Dioxide from Nitrogen or Methane by Supported Ionic Liquid Membranes (SILMs): Influence of the Cation Charge of the Ionic Liquid. *J. Phys. Chem. B* **2013**, *117*, 15131−15140.

(19) Yeganegi, S.; Soltanabadi, A.; Farmanzadeh, D. Molecular Dynamic Simulation of Dicationic Ionic Liquids: Effects of Anions and Alkyl Chain Length on Liquid Structure and Diffusion. *J. Phys. Chem. B* **2012**, *116*, 11517−11526.

(20) Lopes, J. N. C.; Deschamps, J.; Padua, A. A. H. Modeling Ionic Liquids Using a Systematic All-Atom Force Field. *J. Phys. Chem. B* **2004**, *108*, 2038−2047.

(21) Arora, G.; Sandler, S. I. Air Separation by Single Wall Carbon Nanotubes: Mass Transport and Kinetic Selectivity. *J. Chem. Phys.* **2006**, *124*, 084702.

(22) Hess, B.; Bekker, H.; Berendsen, H. J. C.; Fraaije, J. G. E. M. Lincs: A Linear Constraint Solver for Molecular Simulations. *J. Comput. Chem.* **1997**, *18*, 1463−1472.

(23) Essmann, U.; Perera, L.; Berkowitz, M. L.; Darden, T.; Lee, H.; Pedersen, L. G. A Smooth Particle Mesh Ewald Method. *J. Chem. Phys.* **1995**, *103*, 8577−8593.

(24) Berendsen, H. J. C.; Vanderspoel, D.; Vandrunen, R. Gromacs - a Message-Passing Parallel Molecular-Dynamics Implementation. *Comput. Phys. Commun.* **1995**, *91*, 43−56.

(25) Frisch, M. J.; Trucks, G. W.; Schlegel, H. B.; Scuseria, G. E.; Robb, M. A.; Cheeseman, J. R.; Scalmani, G.; Barone, V.; Mennucci, B.; Petersson, G. A.; Nakatsuji, H.; Caricato, M.; Li, X.; Hratchian, H. P.; Izmaylov, A. F.; Bloino, J.; Zheng, G.; Sonnenberg, J. L.; Hada, M.; Ehara, M.; Toyota, K.; Fukuda, R.; Hasegawa, J.; Ishida, M.; Nakajima, T.; Honda, Y.; Kitao, O.; Nakai, H.; Vreven, T.; Montgomery, J. A.; Peralta, J. E.; Ogliaro, F.; Bearpark, M.; Heyd, J. J.; Brothers, E.; Kudin, K. N.; Staroverov, V. N.; Keith, T.; Kobayashi, R.; Normand, J.; Raghavachari, K.; Rendell, A.; Burant, J. C.; Iyengar, S. S.; Tomasi, J.; Cossi, M.; Rega, N.; Millam, J. M.; Klene, M.; Knox, J. E.; Cross, J. B.; Bakken, V.; Adamo, C.; Jaramillo, J.; Gomperts, R.; Stratmann, R. E.; Yazyev, O.; Austin, A. J.; Cammi, R.; Pomelli, C.; Ochterski, J. W.;

DOI: 10.1021/la5048563
Langmuir XXXX, XXX, XXX−XXX

Martin, R. L.; Morokuma, K.; Zakrzewski, V. G.; Voth, G. A.; Salvador, P.; Dannenberg, J. J.; Dapprich, S.; Daniels, A. D.; Farkas, O.; Foresman, J. B.; Ortiz, J. V.; Cioslowski, J.; Fox, D. J. *Gaussian 09, Revision D.01*; Gaussian, Inc.: Wallingford, CT, 2013.

(26) Boys, S. F.; Bernardi, F. The Calculation of Small Molecular Interactions by the Differences of Separate Total Energies. Some Procedures with Reduced Errors. *Mol. Phys.* **1970**, *19*, 553−566.

(27) Aparicio, S.; Atilhan, M. On the Properties of CO_2 and Flue Gas at the Piperazinium-Based Ionic Liquids Interface: A Molecular Dynamics Study. *J. Phys. Chem. C* **2013**, *117*, 15061−15074.

(28) Yan, T.; Li, S.; Jiang, W.; Gao, X.; Xiang, B.; Voth, G. A. Structure of the Liquid-Vacuum Interface of Room-Temperature Ionic Liquids: A Molecular Dynamics Study. *J. Phys. Chem. B* **2006**, *110*, 1800−1806.

(29) Lynden-Bell, R. M.; Del Popolo, M. Simulation of the Surface Structure of Butylmethylimidazolium Ionic Liquids. *Phys. Chem. Chem. Phys.* **2006**, *8*, 949−954.

(30) Bhargava, B. L.; Balasubramanian, S. Layering at an Ionic Liquid-Vapor Interface: A Molecular Dynamics Simulation Study of [Bmim][PF_6]. *J. Am. Chem. Soc.* **2006**, *128*, 10073−10078.

(31) Perez-Blanco, M. E.; Maginn, E. J. Molecular Dynamics Simulations of CO_2 at an Ionic Liquid Interface: Adsorption, Ordering, and Interfacial Crossing. *J. Phys. Chem. B* **2010**, *114*, 11827−11837.

(32) Moganty, S. S.; Chinthamanipeta, P. S.; Vendra, V. K.; Krishnan, S.; Baltus, R. E. Structure-Property Relationships in Transport and Thermodynamic Properties of Imidazolium Bistriflamide Ionic Liquids for CO_2 Capture. *Chem. Eng. J.* **2014**, *250*, 377−389.

(33) Shirota, H.; Mandai, T.; Fukazawa, H.; Kato, T. Comparison between Dicationic and Monocationic Ionic Liquids: Liquid Density, Thermal Properties, Surface Tension, and Shear Viscosity. *J. Chem. Eng. Data* **2011**, *56*, 2453−2459.

(34) Li, S.; Banuelos, J. L.; Zhang, P.; Feng, G.; Dai, S.; Rother, G.; Cummings, P. T. Toward Understanding the Structural Heterogeneity and Ion Pair Stability in Dicationic Ionic Liquids. *Soft Matter* **2014**, *10*, 9193−9200.

(35) Anthony, J. L.; Anderson, J. L.; Maginn, E. J.; Brennecke, J. F. Anion Effects on Gas Solubility in Ionic Liquids. *J. Phys. Chem. B* **2005**, *109*, 6366−6374.

DOI: 10.1021/la5048563
Langmuir XXXX, XXX, XXX−XXX